nature astronomy

ARTICLES

https://doi.org/10.1038/s41550-019-0906-9

Planck evidence for a closed Universe and a possible crisis for cosmology

Eleonora Di Valentino[1], Alessandro Melchiorri[2*] and Joseph Silk[3,4,5]

The recent Planck Legacy 2018 release has confirmed the presence of an enhanced lensing amplitude in cosmic microwave background power spectra compared with that predicted in the standard Λ cold dark matter model, where Λ is the cosmological constant. A closed Universe can provide a physical explanation for this effect, with the Planck cosmic microwave background spectra now preferring a positive curvature at more than the 99% confidence level. Here, we further investigate the evidence for a closed Universe from Planck, showing that positive curvature naturally explains the anomalous lensing amplitude, and demonstrating that it also removes a well-known tension in the Planck dataset concerning the values of cosmological parameters derived at different angular scales. We show that since the Planck power spectra prefer a closed Universe, discordances higher than generally estimated arise for most of the local cosmological observables, including baryon acoustic oscillations. The assumption of a flat Universe could therefore mask a cosmological crisis where disparate observed properties of the Universe appear to be mutually inconsistent. Future measurements are needed to clarify whether the observed discordances are due to undetected systematics, or to new physics or simply are a statistical fluctuation.

The recent Planck Legacy 2018 (PL18) release of observations of cosmic microwave background (CMB) anisotropies has reported some unexpected results, revealing the possibility for new physics beyond the standard Λ cold dark matter (ΛCDM) model, where Λ is the cosmological constant[1,2]. Indeed, while the inflationary predictions for coherent acoustic oscillations have been fully confirmed, a preference for a higher lensing amplitude, $A_{\rm lens}$, than predicted in the base ΛCDM model at about 3 standard deviations has been found in the temperature and polarization angular spectra. We argue that the $A_{\rm lens}$ anomaly has profound implications for some extensions to the ΛCDM model, such as the curvature of the Universe. The constraints from the PL18 CMB spectra on curvature, parameterized through the energy density parameter Ω_K, are indeed surprising, suggesting a closed Universe at 3.4 standard deviations ($-0.007>\Omega_K>-0.095$ at the 99% confidence level (CL)[1–3]).

As is well known, inflation theory naturally predicts a flat Universe[4,5]. However, inflationary models with $\Omega_K<0$ (refs. [6–8]) are relatively simple to build, with primordial homogeneity and isotropy easier to achieve than in open models. An issue for closed inflation models is that to obtain $\Omega_K\approx-0.1$, fine-tuning at a level of a few per cent is needed[7]. This does not sound very compelling, but it may still be acceptable, given the presence of a far more finely tuned cosmological constant. Closed models could also lead to a large-scale cut-off in the primordial density fluctuations, around the curvature scale $R_c=(c/H_0)|\Omega_K|^{0.5}\approx 1\,\mathrm{Gpc}$ (where R_c is the curvature radius, c is the velocity of light and H_0 is the current value of the Hubble constant), in agreement with the observed low CMB anisotropy quadrupole[7,9]. Confirmation of a positive spatial curvature would also have several implications for inflationary theory and, for example, severely challenge models of eternal inflation[10,11].

Here, we show that, if indeed credible, the Planck preference for a closed Universe introduces a new problem for modern cosmology. Indeed, many of the current tight constraints on cosmological parameters are obtained by combining complementary datasets. A basic assumption in this procedure is that these different datasets must be consistent, that is, they must plausibly arise from the same cosmological model. Currently, two major experimental datasets are in tension with Planck: the determination of the Hubble constant by Riess et al.[12] is discrepant at the level of ~3 standard deviations (but see also ref. [13]), and the observations of cosmic shear by the Kilo Degree Survey 450 (KiDS-450) disagree at ~2 standard deviations[14,15]. Furthermore, the value of $A_{\rm lens}$ derived from the Planck lensing-generated four-point correlation function is consistent with the expectations of the ΛCDM model and in tension with the PL18 power spectra[1,16].

Although most of the remaining cosmological observables are considered to be in good agreement with PL18, these inconsistencies have already motivated several studies that have attempted to critically reassess the level of discordance[17–19] or to resolve it with the introduction of new physics[20–24].

The level of accordance between cosmological observables has hitherto been thoroughly investigated under the assumption of a flat Universe. We show here that when curvature is allowed to vary (as suggested by the PL18 CMB spectra), the statistical significance of the known tensions with PL18 increases and other discrepancies arise with several 'local' (at redshift $z<3$) observables. The assumption of a flat Universe could, therefore, mask a cosmological crisis where disparate observed properties of the Universe appear to be mutually inconsistent.

Before evaluating the tensions of the PL18 results with independent cosmological observables, we first check whether the PL18 power spectra can provide an unbiased and reliable estimate of the curvature of the Universe. This may not be the case, since 'geometrical degeneracy' is present between cosmological parameters[25–27]. For example, assuming the same inflationary parameters and

[1]Jodrell Bank Centre for Astrophysics, School of Physics and Astronomy, University of Manchester, Manchester, UK. [2]Physics Department and INFN, Università di Roma 'La Sapienza', Rome, Italy. [3]Institut d'Astrophysique de Paris (UMR7095: CNRS & UPMC, Sorbonne Universities), Paris, France. [4]Department of Physics and Astronomy, The Johns Hopkins University, Baltimore, MD, USA. [5]BIPAC, Department of Physics, University of Oxford, Oxford, UK. *e-mail: alessandro.melchiorri@uniroma1.it

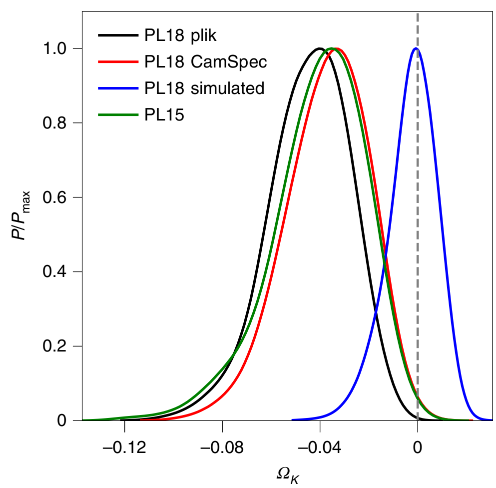

Fig. 1 | Preference for a closed Universe, $\Omega_K<0$, from Planck. Posterior (P) distributions normalized at the maximum value (P_{max}) for Ω_K from PL18 temperature and polarization-simulated angular power spectra (assuming a fiducial flat ΛCDM model) and PL18 real data, adopting the baseline 'Plik' Planck likelihood and the alternative 'CamSpec' likelihood, respectively. For comparison, the posterior from the previous PL15[34] data release is also shown.

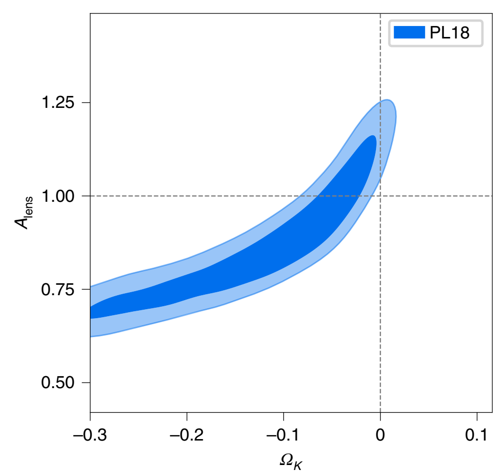

Fig. 2 | Degeneracy between curvature and lensing. Constraints at 68% (dark blue) and 95% (light blue) CLs in the A_{lens} versus Ω_K plane from PL18 temperature and polarization data. A degeneracy between curvature and the A_{lens} parameter is clearly present. Note that a model with $\Omega_K<0$ is slightly preferred with respect to a flat model with $A_{lens}>1$.

reionization process, a flat cosmological model with matter density $\Omega_m=0.35$, cosmological constant density $\Omega_\Lambda=0.65$ and $H_0=65\,\mathrm{km\,s^{-1}\,Mpc^{-1}}$ produces an identical structure of the CMB angular spectrum at subdegree angular scales for a closed model with $\Omega_m=1$, $\Omega_\Lambda=0.15$ (that is, $\Omega_K=-0.15$) and $H_0=38.4\,\mathrm{km\,s^{-1}\,Mpc^{-1}}$. Because of the form of the degeneracy, different closed models have identical CMB power spectra to that of a single flat model. The main consequence is that, after marginalization over the nuisance parameters, the posterior on Ω_K is generally skewed towards closed models[28].

The situation changes with precise CMB measurements at arc minute angular scales: here, indeed, additional anisotropies induced by gravitational lensing are not negligible. Since gravitational lensing depends on the matter density, its detection breaks the geometrical degeneracy. The Planck experiment, with its improved angular resolution, therefore offers the opportunity of a precise measurement of curvature from a single CMB experiment.

To confirm this hypothesis, we generated a Monte Carlo Markov chain (MCMC) analysis over simulated Planck (temperature and polarization) data, assuming the best-fit flat ΛCDM model and experimental noise properties similar to those presented in the PL18 release[1]. As we can see from Fig. 1, the expected posterior is centred around $\Omega_K=0$, with a bound of $\Omega_K=0.00\pm0.02$ at the 68% CL. Potentially, an experiment such as Planck could constrain curvature with ~2% uncertainty, without any substantial bias towards closed models.

For comparison, in Fig. 1, we have plotted the posterior from the PL18 real temperature and polarization power spectra, assuming the baseline Planck likelihood (see ref. [2]). As we can see, the posterior is reasonably centred on a closed model around $\Omega_K=-0.04$. Integrating this posterior distribution over Ω_K, we find that Planck favours a closed Universe ($\Omega_K<0$) with 99.985% probability. Moreover, a closed Universe with $\Omega_K=-0.0438$ provides a better fit to PL18 with respect to a flat model, with a χ^2 difference of $\Delta\chi^2_{\rm eff}\approx-11$, where $\chi^2_{\rm eff}$ is the effective best-fit chi squared from the MCMC chains[3].

This qualitatively shows the PL18 preference for a closed Universe, but does not statistically weight the additional parameter (Ω_K). To better quantify the preference for a closed model, we adopt the deviance information criterion (DIC)[29–31], which takes into account the Bayesian complexity, that is, the effective number of parameters, of the extended model[30] and is defined as

$$\mathrm{DIC}=2\overline{\chi^2_{\rm eff}}-\chi^2_{\rm eff} \tag{1}$$

where the bar denotes a mean over the posterior distribution. This quantity can be easily computed. We restrict the analysis to models with curvature in the range $-0.2\le\Omega_K\le0$; that is, we neglect open models because they are both disfavoured from observations and more difficult to realize in an inflationary scenario. We find that the Planck data yield $\Delta\mathrm{DIC}=-7.4$; that is, a closed Universe with $\Omega_K=-0.0438$ is preferred, with a probability ratio of about 1/41, with respect to a flat model.

We also compute the Bayesian evidence ratio by making use of the Savage–Dickey density ratio[30,32,33]. Assuming the Savage–Dickey density ratio, the Bayes factor B_{01} can be written as

$$B_{01}=\left.\frac{p(\Omega_K|d,M_1)}{\pi(\Omega_K|M_1)}\right|_{\Omega_K=0} \tag{2}$$

where M_1 denotes the model with curvature, $p(\Omega_K|d,M_1)$ is the posterior for Ω_K in this theoretical framework, computed from a specific dataset d, and $\pi(\Omega_K|M_1)$ is the prior on Ω_K that we assume to be flat in the range $-0.2\le\Omega_K\le0$.

Applying the Savage–Dickey method to the Planck temperature and polarization, we obtain the Bayes ratio of

$$|\ln B_{01}|=3.3 \tag{3}$$

that is, by assuming the so-called Jeffreys's scale, we obtain strong evidence for closed models with Ω_K in the prior range $[-0.2,0]$. While the assumption of a larger prior would lead to weaker evidence, the preference from the data for a closed Universe is clear.

This evidence could come from an unidentified systematic in the Planck data. However, as we can also see from the posteriors in Fig. 1, the preference for a closed Universe increases as we move from the Planck 2015 (PL15)[34] data release to the current PL18 release. Moreover, even assuming a significantly different procedure for the likelihood analysis[2], and using the alternative CamSpec approach instead of the baseline Planck likelihood, the preference for

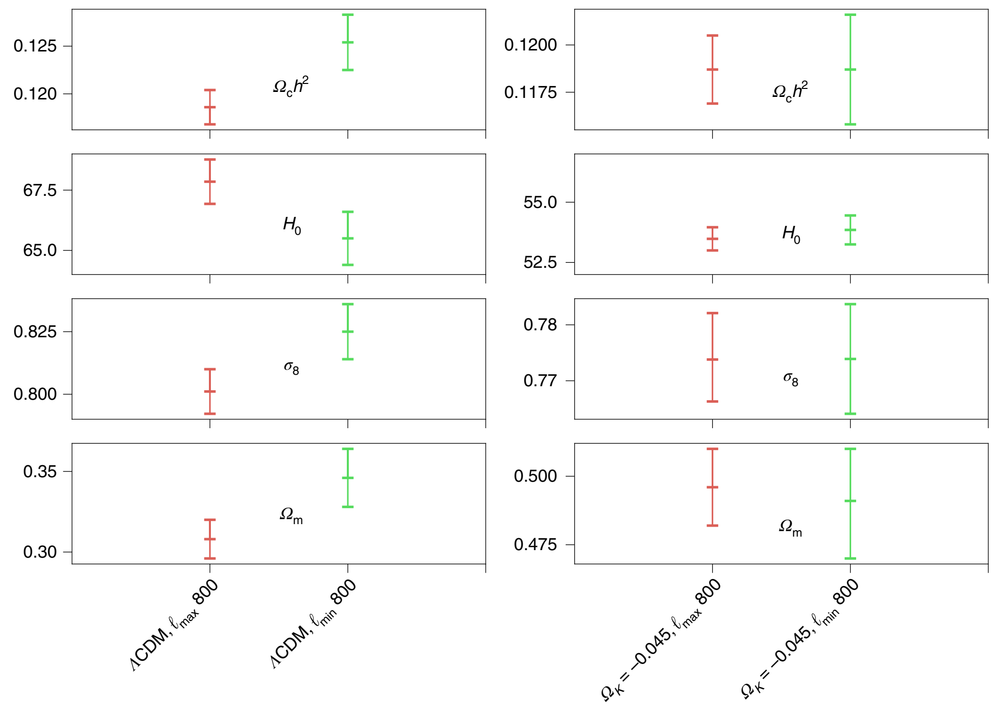

Fig. 3 | Curvature and shift in parameters. Constraints at 68% CL on cosmological parameters derived from two different multipole ranges ($2 \leq \ell \leq 800$ and $800<\ell \leq 2{,}500$) of the PL18 temperature and polarization data, assuming either a ΛCDM model (left) or a closed model (right). Polarization data at low multipoles ($2 \leq \ell \leq 30$) are included in both cases. The difference in the parameter constraints, present in flat ΛCDM, disappears when assuming a model with $\Omega_K = -0.045$. The parameters for each panel are non-dimensional with the exception of H_0 which has units of km s^{-1} Mpc^{-1}. l_{max}, maximum l; l_{min}, minimum l.

curvature is reduced, but is still well above 2 standard deviations with $\Omega_K = -0.037^{+0.032}_{-0.034}$ at the 95% CL[3]. In the case of CamSpec, we find $\Omega_K < 0$ with a 99.85% probability. Although the indication for a closed Universe is less significant with CamSpec, it is still present, showing that our result is not due to differences between analysis methods.

The preference for closure in the Planck data is strongly connected to the higher lensing amplitude. This is evident from the parameter degeneracy between A_{lens} and Ω_K, as shown in Fig. 2, where we report the two-dimensional (2D) constraints at 68% and 95% CLs on A_{lens} and Ω_K from the PL18 temperature and polarization data[2]. The dark matter content can indeed be greater in a closed Universe, leading to a larger lensing signal, solving the A_{lens} anomaly and providing a robust physical explanation. As we can see, when a closed model is considered, A_{lens} is in agreement with the expectation of $A_{lens} = 1$. The amplitude of the lensing signal in Planck temperature and polarization data is precisely what is expected in a closed Universe. It is interesting to note that a ΛCDM + Ω_K analysis provides a marginally better fit to the ΛCDM + A_{lens} analysis, by $\Delta\chi^2 = -1.6$, because closed models better fit the low-multipole data.

As discussed in ref. [35], assuming a flat ΛCDM model, the values of the cosmological parameters obtained from the PL15 temperature angular spectrum in the multipole range $2 \leq \ell \leq 800$ are 'shifted' with respect to those derived from the same Planck data relative to multipoles in the range $800 < \ell \leq 2{,}500$. This tension is also present in the PL18 release[2], and the inclusion of the A_{lens} parameter removes this difference. A key point of our paper is that the addition of curvature also solves this tension: in Fig. 3, we show that in a closed Universe with $\Omega_K = -0.045$, the cosmological parameters derived in the two different multipole ranges, from PL18 temperature and polarization data, are now fully compatible.

However, if the PL18 power spectra suggest a closed Universe, the remaining cosmological observables are in strong disagreement with this. Let us now compare the Planck constraints with those coming from local observables, starting with baryon acoustic oscillations. We first consider a combination of measurements given by the Six-degree Field Galaxy Survey (6dFGS)[36], Sloan Digital Sky Survey–Main Galaxy Sample (SDSS-MGS)[37] and Baryon Oscillation Spectroscopic Survey Data Release 12 (BOSS DR12)[38] (hereafter, we refer to this dataset simply as BAO, where BAO stands for baryon acoustic oscillations), as adopted by the Planck Collaboration[1]. The combination of this BAO dataset and PL18 power spectra produces a strong constraint on curvature, with $\Omega_K = 0.0008^{+0.0038}_{-0.0037}$ at the 95% CL[1], in excellent agreement with a flat Universe. Given the significant change in the conclusions from Planck alone, it is reasonable to investigate whether the BAO dataset is actually consistent with PL18. The level of concordance between the Planck and BAO data, even from a qualitative point of view, is immediately clear from Fig. 4, where we plot the acoustic-scale distance ratio, $D_V(z)/r_{drag}$, as a function of redshift, taken from several recent BAO surveys, and divided by the mean acoustic-scale ratio obtained by Planck temperature and polarization data adopting a ΛCDM + Ω_K model. Here, r_{drag} is the comoving size of the sound horizon at the time of the end of the baryon drag epoch, and D_V, the dilation scale, is a combination of the Hubble parameter $H(z)$ and the comoving angular diameter distance $D_M(z)$: $D_V(z) = (czD_M^2(z)/H(z))^{1/3}$. As we see, there is a striking disagreement between the PL18 power spectra and the BAO data. This can also be seen in Table 1, where we report the constraints on D_M and $H(z)$ from the recent analysis of BOSS DR12 data[38] and the corresponding constraints obtained indirectly from Planck, assuming a ΛCDM model with curvature. Each of

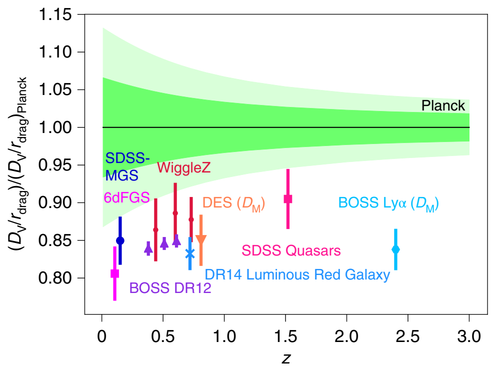

Fig. 4 | Tension with BAO. Acoustic-scale distance (D_V) measurements divided by the corresponding mean distance ratio from PL18 temperature and polarization power spectra in a ΛCDM + Ω_K model. The green bands show the 68% (dark green) and 95% (light green) confidence ranges. The data points correspond to the measurements at the 68% CL from the following experiments: 6dFGS[36], SDSS-MGS[37] and BOSS DR12[38] (the BAO dataset considered in this paper). We also report measurements from WiggleZ[53], the DES[40,54], the DR14 Luminous Red Galaxy sample[55], SDSS Quasars[56] and BOSS Lyα[57].

Table 1 | Comoving angular diameter distances D_M (corrected by the fiducial comoving sound horizon r_d at the baryon drag epoch assumed in the survey's analysis ($r_{d,fid}$)) and Hubble parameter measurements from recent BAO observations from BOSS DR12[38] compared with the corresponding quantities derived from PL18 power spectra assuming a ΛCDM + Ω_K model

Observable	Redshift	BAO (68% CL)	Planck (68% CL)	Tension
$D_M(r_{d,fid}/r_d)$ (Mpc)	0.38	1,518 ± 22.8	1,843 ± 100	2.9σ
$D_M(r_{d,fid}/r_d)$ (Mpc)	0.51	1,977 ± 26.9	2,361 ± 115	3.0σ
$D_M(r_{d,fid}/r_d)$ (Mpc)	0.61	2,283 ± 32.3	2,726 ± 130	3.3σ
$H(r_{d,fid}/r_d)$ (km s^{-1} Mpc^{-1})	0.38	81.5 ± 1.9	71.6 ± 3.3	2.6σ
$H(r_{d,fid}/r_d)$ (km s^{-1} Mpc^{-1})	0.51	90.5 ± 1.97	78.9 ± 3.1	3.1σ
$H(r_{d,fid}/r_d)$ (km s^{-1} Mpc^{-1})	0.61	97.3 ± 2.1	85.0 ± 3.0	3.3σ

the BOSS DR12 data points is in disagreement by about 3 standard deviations with the Planck power spectra.

As we can see from Table 2, the PL18 $\chi^2_{\rm eff}$ best fit is worse by $\Delta\chi^2 \approx 16.9$ when the BAO data are included[3] under the assumption of curvature. This is a significantly larger $\Delta\chi^2$ than obtained for the case of ΛCDM ($\Delta\chi^2 \approx 6.15$). The BAO dataset that we adopted consists of two independent measurements (6dFGS[36] and SDSS-MGS[37]) with relatively large error bars (that is, with low statistical weight; see Fig. 4), and six correlated measurements from BOSS DR12[38]. It is therefore not straightforward to determine the number of independent data points present in the BAO dataset and to estimate the disagreement between the datasets from a simple χ^2 analysis. Although several statistical methods have been proposed to quantify the discrepancy between two cosmological datasets[17–19], here, we check for consistency between two independent datasets, D_1 and D_2, by evaluating the following quantity based on the DIC approach[14,15]:

$$\mathcal{I}(D_1, D_2) \equiv \exp\{-\mathcal{F}(D_1, D_2)/2\} \quad (4)$$

Table 2 | Tensions between PL18 and BAO and CMB lensing

Additional dataset	$\Delta\chi^2_{\rm eff}$	$\Delta N_{\rm data}$	$\log_{10}\mathcal{I}$
flat ΛCDM			
+ BAO	+6.15	8	0.2
+ CMB lensing	+8.9	9	0.6
ΛCDM + Ω_K			
+ BAO	+16.9	8	−1.8
+ CMB lensing	+16.9	9	−0.84

In the second column, we report the best-fit $\Delta\chi^2_{\rm eff}$ with respect to the PL18 dataset alone. In the third column is the number $\Delta N_{\rm data}$ of (correlated) experimental data points from the additional dataset. In the fourth column is the value of $\log_{10}\mathcal{I}$ that quantifies the tension (substantial if less than −0.5, strong if less than −1.0). We note good agreement between the datasets in the case of flat ΛCDM. In contrast, statistically significant tensions arise when curvature is considered.

where

$$\mathcal{F}(D_1, D_2) = {\rm DIC}(D_1 \cup D_2) - {\rm DIC}(D_1) - {\rm DIC}(D_2) \quad (5)$$

where ${\rm DIC}(D_1 \cup D_2)$ is the DIC obtained from the combined analysis of the two datasets.

Following the Jeffreys's scale, the agreement/disagreement is considered 'substantial' if $|\log_{10}\mathcal{I}| > 0.5$, 'strong' if $|\log_{10}\mathcal{I}| > 1.0$ and 'decisive' if $|\log_{10}\mathcal{I}| > 2.0$. When $\log_{10}\mathcal{I}$ is positive, then two datasets are in agreement, whereas they are in tension if this parameter is negative. We show in Table 2 the values of $\log_{10}\mathcal{I}$ computed for the PL18 (D_1) and BAO (D_2) datasets in the case of ΛCDM and ΛCDM + Ω_K. For the ΛCDM model, there is reasonable agreement between the datasets ($\log_{10}\mathcal{I} = 0.2$), but evaluating models with curvature results in strong disagreement $\log_{10}\mathcal{I} = -1.8$) between Planck and BAO data.

A second tension is present between PL18 power spectra and the constraints on the lensing potential derived from the four-point function of Planck CMB maps[39] (hereafter, called CMB lensing). Indeed, as discussed previously, the preference for $\Omega_K < 0$ in PL18 is mostly due to the anomalous lensing amplitude at small angular scales[1]. However, this greater lensing amplitude is not seen in the CMB lensing data, which is consistent with a flat ΛCDM model. This can be seen in Fig. 5, where we compare the lensing-potential power spectra best fits from the PL18 power spectra, obtained under the assumptions of curvature or flatness, with the CMB lensing data[39]. The flat ΛCDM model is in reasonable agreement with CMB lensing, while the PL18 best-fit $\Omega_K = -0.0438$ model predicts a too large lensing amplitude (with the exception of two data points). As we can see from Fig. 4, the PL18 power spectra best-fit closed model predicts a lensing-potential spectrum that is very similar to the best fit obtained under ΛCDM + $A_{\rm lens}$ with $A_{\rm lens} = 1.191$ (ref. [3]).

A PL18 + CMB lensing analysis yields $\Omega_K = 0.011^{+0.013}_{-0.012}$ at the 95% CL, bringing a flat Universe back into agreement within 2 standard deviations, but still also suggesting preference for a closed Universe. However, it is interesting to quantify the discordance between PL18 and CMB lensing. As we can see in Table 2, the inclusion of CMB lensing in PL18 increases the best-fit chi squared by $\Delta\chi^2 = 16.9$ in the case of ΛCDM + Ω_K (while in the case of the ΛCDM model, we have $\Delta\chi^2 = 8.9$). The CMB lensing dataset consists of nine correlated data points. Even assuming these data points to be independent, the increase in χ^2 when curvature is varied suggests there is tension at the 95% CL, while there is no significant tension in the case of flatness. Also in Table 2, we report the values of the $\mathcal{I}$ quantity. We identify substantial agreement between PL18 and CMB lensing in the case of a flat Universe ($\log_{10}\mathcal{I} = 0.6$) that changes to substantial discordance ($\log_{10}\mathcal{I} = -0.84$) when curvature is allowed to vary.

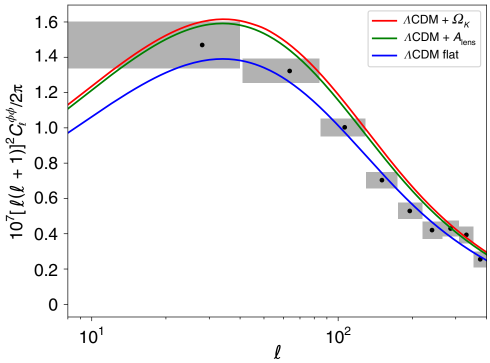

Fig. 5 | Tension with CMB lensing. The solid lines are the theoretical predictions for the best-fits CMB lensing power spectra $\left(C_\ell^{\phi\phi}\right)$ from the PL18 angular spectra in the case of ΛCDM, ΛCDM + Ω_K and ΛCDM + A_{lens} models, respectively. The ΛCDM + Ω_K model has $\Omega_K = -0.0438$, while the flat ΛCDM + A_{lens} model has $A_{\mathrm{lens}} = 1.191$. The grey bands (errors at 68% CL) are the CMB lensing conservative experimental band powers extracted from the PL18 trispectrum data, while the black dots are the measured values.

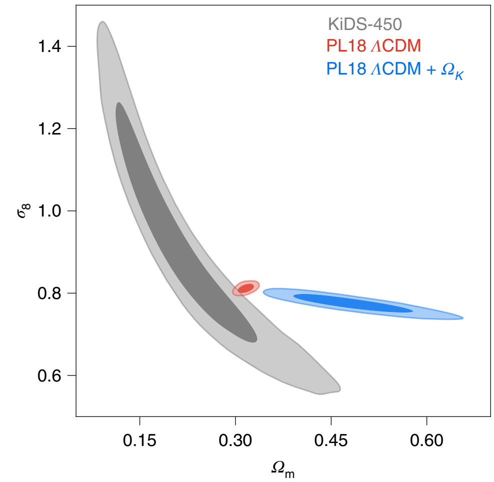

Fig. 6 | Tension with cosmic shear measurements. Discordance between PL18 and the KiDS-450 cosmic shear survey in the σ_8 versus Ω_m plane. Darker shaded areas show constraints at 68% CL while lighter shaded areas show constraints at 95% CL. The tension already present under flat ΛCDM (at about 2.3 standard deviations) is increased to more than 3.5 standard deviations when curvature is incorporated into the analysis of PL18.

In conclusion, if the assumption of a flat Universe is removed and curvature is permitted, as preferred by the PL18 power spectra, we find strong disagreement between Planck and BAO data, and substantial disagreement between Planck and CMB lensing data.

It is interesting to investigate whether astrophysical measurements that are already in tension with Planck under the assumption of a flat Universe are still in disagreement when curvature is considered. In a ΛCDM + Ω_K model, PL18 power spectra provide the constraint: $H_0 = 54.4^{+3.3}_{-4.0}$ at the 68% CL[3]. This is now in tension at the level of 5.2 standard deviations with respect to the conservative constraint of $H_0 = 73.52 \pm 1.62$ at the 68% CL from the Riess et al.[12] analysis (R18). The inclusion of curvature, therefore, significantly increases (by ~48%) the tension between Planck and R18.

A similar increase in the tension is present with cosmic shear data from KiDS-450. In Fig. 6, we show the 2D constraints in the σ_8, the amplitude of mass fluctuations, versus Ω_m plane from KiDS-450 and PL18 power spectra under the assumption of curvature. For comparison, we also include the Planck constraint under flat ΛCDM (the KiDS-450 bound is just slightly different when flatness is assumed). As we can see, there is a significant shift in this plane for the PL18 constraint when moving from a flat to a closed Universe, which increases the discrepancy with KiDS-450. Considering $S_8 = \sigma_8(\Omega_m/0.3)^{0.5}$, from the PL18 power spectra, we obtain $S_8 = 0.981 \pm 0.049$ at the 68% CL, a value that is now about 3.8 standard deviations from the KiDS-450 result. Cosmic shear measurements have also recently been made by the Dark Energy Survey (DES)[40] and by the Subaru Hyper Suprime-Cam (HSC)[41]. These measurements are reasonably consistent with the PL18 result in a flat Universe. However, assuming that the reported constraint on the S_8 parameter depends weakly on Ω_K, we find that once curvature is allowed, the PL18-derived determination of S_8 is discordant at more than 3.5 standard deviations with the DES and at more than 3 standard deviations with the HSC. In practice, when curvature is included, not only the significance of the tension with KiDS-450 increases, but PL18 is now also significantly discordant with recent cosmic shear surveys such as the DES and HSC.

Until now, we have studied the compatibility of single datasets with PL18. However, analyses are usually performed by combining multiple datasets. It is therefore interesting to address the compatibility of Planck with combined datasets. In Fig. 7, we show the confidence region at the 95% CL from a BAO + SNe-Ia + BBN dataset (where SNe-Ia refers to type-Ia supernovae and BBN to big bang nucleosynthesis) and the 68% and 95% CLs from the PL18 power spectra on the Ω_K versus H_0 plane. As we can see, there is strong tension between the Planck result and that from the combined BAO + SNe-Ia + BBN analysis. In principle, each dataset prefers a closed Universe, with the BAO + SNe-Ia + BBN dataset providing just an upper limit of $\Omega_K < -0.124$ at the 68% CL. However, whereas the Planck result prefers $H_0 = 54^{+3.3}_{-4.0}\,\mathrm{km\,s^{-1}\,Mpc^{-1}}$ at the 68% CL, we find that the BAO + SNe-Ia + BBN dataset gives $H_0 = 79.6 \pm 6.8\,\mathrm{km\,s^{-1}\,Mpc^{-1}}$ at the 68% CL; that is, they are inconsistent at the level of 3.4 standard deviations. Moreover, the BAO + SNe-Ia + BBN data prefer lower ages of the Universe (t_0), with $t_0 = 11.73^{+0.92}_{-1.3}$ Gyr at the 68% CL, which is in modest tension with the recent age determinations (t_*) of the stars 2MASS J18082002–5104378 B (ref. [42]) and HD 140283, of $t_* = 13.535 \pm 0.002$ Gyr and $t_* = 13.5 \pm 0.7$ Gyr (refs. [43,44]), respectively.

As we can see from Fig. 7, the probability contour plots from the BAO + SNe-Ia + BBN analysis are rather broad. It is therefore interesting to include further observables to improve the constraints. We consider, separately, CMB lensing, the R18 determination of the Hubble constant and the observed angular size of the sound horizon at recombination, $\theta_{\mathrm{MC}} = 1.04116 \pm 0.00033$ (where the subscript MC stands for Monte Carlo), in a ΛCDM + Ω_K model from PL18. We show the results of this kind of analysis in Fig. 8. The inclusion of the θ_{MC} prior from Planck shifts the constraints towards a flat ΛCDM model with $\Omega_K = 0.0016 \pm 0.0075$ at the 68% CL. The inclusion of the CMB lensing dataset also significantly improves the constraints, with $\Omega_K = 0.00 \pm 0.01$ at the 68% CL. Both BAO + SNe-Ia + BBN + θ_{MC} and BAO + SNe-Ia + CMB lensing combinations provide evidence for a flat Universe, with good consistency between the datasets. We may argue that when deriving constraints under the assumption of a flat Universe, it would be more conservative to use these data combinations instead of PL18, since they are consistent with a flat ΛCDM model and do not show significant internal tensions. However, these data combinations still show a significant discordance with PL18 power spectra. Considering the parameter constraints derived from the BAO + SNe-Ia + CMB lensing dataset, we indeed find disagreement with PL18 at 2.4 standard deviations in Ω_K, amounting to 2.7 standard deviations in H_0, and 2.9 standard deviations in S_8. When we consider the combination of BAO + SNe-Ia + BBN + R18,

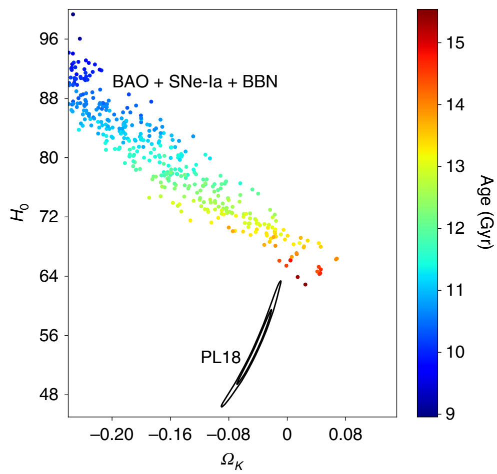

Fig. 7 | Tension with combined data. Contour plots at 68% (inner contour) and 95% (outer contour) CLs from PL18 and 95% CL region from BAO + SNe-Ia + BBN datasets in the H_0 versus Ω_K plane and as a function of the age of the Universe.

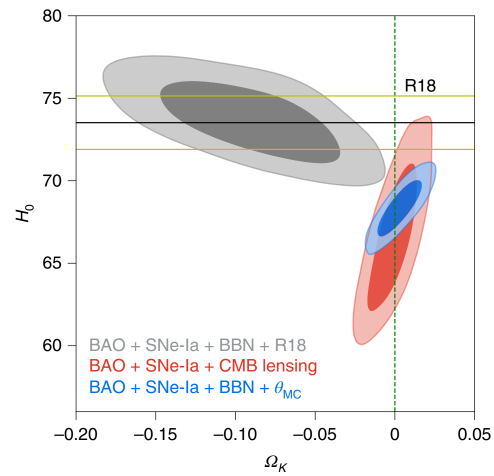

Fig. 8 | Tensions in combined data. Contour plots at 68% and 95% CLs (dark shading and light shading, respectively) from the BAO + SNe-Ia + BBN + H_0, BAO + SNe-Ia + BBN + θ_{MC} and BAO + SNe-Ia + CMB lensing datasets in the Ω_K versus H_0 plane. Also shown are the constraints on the Hubble constant from R18[12]. The black line is the mean value on Hubble constant from R18 and the yellow lines delimit the 68% CL region.

we find $\Omega_K = -0.091 \pm 0.037$ at the 68% CL, which, again, provides an indication of a closed Universe (see Fig. 8). Both datasets provide good best-fit chi-squared values, and it is impossible to discriminate one result over another from the statistical point of view. As we can see from Fig. 8, there is good agreement between the BAO + SNe-Ia + CMB lensing and BAO + SNe-Ia + BBN + θ_{MC} datasets, while both are in significant tension at the level of 2.5 standard deviations with BAO + SNe-Ia + BBN + R18.

In summary, the PL18 CMB power spectra provide a statistically significant indication for a closed Universe. A closed Universe solves the internal tensions present in the Planck dataset on the value of the cosmological parameters derived at different angular scales. Positive curvature is also marginally suggested by the ages of the oldest stars (see, for example, refs. [42,43]) and, in a combined analysis with the A_{lens} parameter, slightly favoured by the low CMB quadrupole.

Apart from these arguments, none of the local cosmological observables currently favour a closed Universe, and most of them are consequently in significant discordance with PL18. BAO surveys disagree at more than 3 standard deviations. CMB lensing is in tension at the 95% CL. The R18 constraint on the Hubble constant is in tension with PL18 at more than 5 standard deviations, while cosmic shear data disagree at more than 3 standard deviations.

These inconsistencies between disparate observed properties of the Universe introduce a problem for modern cosmology: the flat ΛCDM model, de facto, does not seem any longer to provide a good candidate for concordance cosmology, given the PL18 power spectra preference for a closed model. At the same time, a closed model is strongly disfavoured by a large number of local observables.

Clearly, a possible solution to this problem would be to speculate about the presence of hitherto undetected systematics in the PL18 release. However, the statistical significance for a closed Universe increases when moving from PL15 to the PL18 release. We point out that the Wilkinson Microwave Anisotropy Probe satellite experiment[28], after nine years of observations, also produced the constraint $\Omega_K = -0.037^{+0.044}_{-0.042}$ at the 68% CL, fully compatible with the Planck result. Finally, we have shown that discordance is also present between the R18 and the CMB lensing datasets once they are both combined with the BAO and SNe-Ia data. In practice, there is currently no supporting evidence that could lead us to believe that the observed inconsistencies are due to systematics in the PL18 data rather than in the low redshift measurements. Moreover, local probes are expected to be more contaminated by astrophysical systematics and/or nonlinearities with respect to CMB anisotropies.

If there are indeed no systematics in the Planck data, then the currently observed discordances may indicate the need for new physics and call for drastic changes in the ΛCDM scenario (see, for example, refs. [21–23,45–47]).

A third possible way is to consider the PL18 constraint on Ω_K as a, now reasonably unlikely, statistical fluctuation. Fortunately, future measurements will fully confirm or falsify current tensions and the PL18 evidence for curvature[48,49]. In the meantime, we argue that the tensions with ΛCDM present in the PL18 release should not be discarded merely as a statistical fluctuation, but must be seriously investigated, since at face value, they point towards a drastic rethinking of the current cosmological concordance model.

Methods

Planck results. Most of the results presented in this paper have been obtained using the publicly accessible PL18 parameter chains, available at http://pla.esac.esa.int/pla/#cosmology.

MCMC analysis. The results in Figs. 1–3 and 6–8 have been obtained by performing an MCMC analysis using the CosmoMC code[50]. All runs have reached a convergence such that $R-1<0.02$, where R is the Raftery–Lewis MCMC diagnostic function. For the Planck data, we considered the recently released PL18 likelihood[2]. The 2D contour plot in Fig. 3 has been obtained assuming an eight-parameter model, where we assume the standard six parameters of the ΛCDM model (baryon density $\Omega_b h^2$ (where h is the reduced Hubble's constant), CDM density $\Omega_c h^2$, primordial amplitude A_s, primordial spectral index n_s, optical depth to reionization τ and sound horizon angular size θ_s) plus Ω_K and A_{lens}. The results in Figs. 7 and 8 are obtained from a BAO + SNe-Ia + BBN dataset, where BAO is the compilation of baryon acoustic oscillations described in the paper, SNe-Ia are the luminosity distances of 1,048 type-Ia supernovae from the recent Pantheon catalogue[51] and BBN is a prior on the baryon density of $\Omega_b h^2 = 0.0222 \pm 0.005$ derived from measurements of primordial deuterium[52] assuming big bang nucleosynthesis.

Figure 3. The results in Fig. 3 have been obtained using the 'clik change lrange bychannel pol.py' tool, publicly available from the PL18 likelihood release[2].

Simulated Planck data. The simulated constraints on Ω_K in Fig. 1 have been obtained using a modified version of the makePerfectForecastDataset.py tool in CosmoMC to match the PL18 ΛCDM constraints.

Planck versus BAO comparison. Figure 4 has been obtained using a modified version of the BAO-data-z.py tool in CosmoMC. The $\log_{10}\mathcal{I}$ quantity has been computed either from the Planck parameter tables available at ref. [3] or from a BAO-only MCMC run.

Data availability

The data that support the plots within this paper and other findings of this study are available at http://pla.esac.esa.int/pla/#cosmology or from the corresponding author upon reasonable request.

Code availability

All of the codes used to produce the presented results are publicly available. See Methods for more details.

Received: 10 March 2019; Accepted: 5 September 2019;
Published online: 04 November 2019

References

1. Aghanim, N. et al. (Planck Collaboration) Planck 2018 results. VI. Cosmological parameters. Preprint at https://arxiv.org/abs/1807.06209 (2018).
2. Aghanim, N. et al. (Planck Collaboration) Planck 2018 results. V. CMB power spectra and likelihoods. Preprint at https://arxiv.org/abs/1907.12875 (2019).
3. *2018 Cosmological Parameters and MC Chains* (Planck Legacy Archive Wiki); https://go.nature.com/2OHvQme
4. Linde, A. D. A new inflationary Universe scenario: a possible solution of the horizon, flatness, homogeneity, isotropy and primordial monopole problems. *Phys. Lett. B* **108**, 389–393 (1982).
5. Albrecht, A. & Steinhardt, P. J. Cosmology for grand unified theories with radiatively induced symmetry breaking. *Phys. Rev. Lett.* **48**, 1220–1223 (1982).
6. Linde, A. D. Inflation with variable Ω. *Phys. Lett. B* **351**, 99–104 (1995).
7. Linde, A. D. Can we have inflation with $\Omega > 1$? *J. Cosmol. Astropart. Phys.* **0305**, 002 (2003).
8. Uzan, J. P., Kirchner, U. & Ellis, G. F. R. Wilkinson Microwave Anisotropy Probe data and the curvature of space. *Mon. Not. Roy. Astron. Soc.* **344**, L65–L68 (2003).
9. Efstathiou, G. Is the low cosmic microwave background quadrupole a signature of spatial curvature? *Mon. Not. Roy. Astron. Soc.* **343**, L95–L98 (2003).
10. Freivogel, B., Kleban, M., Rodríguez Martínez, M. & Susskind, L. Observational consequences of a landscape. *J. High Energy Phys.* **3**, 039 (2006).
11. Guth, A. H. & Nomura, Y. What can the observation of nonzero curvature tell us? *Phys. Rev. D* **86**, 023534 (2012).
12. Riess, A. G. et al. New parallaxes of galactic cepheids from spatially scanning the Hubble Space Telescope: implications for the Hubble constant. *Astrophys. J.* **855**, 136 (2018).
13. Riess, A. G., Casertano, S., Yuan, W., Macri, L. M. & Scolnic, D. Large Magellanic Cloud cepheid standards provide a 1% foundation for the determination of the Hubble constant and stronger evidence for physics beyond ΛCDM. *Astrophys. J.* **876**, 85 (2019).
14. Hildebrandt, H. et al. KiDS-450: cosmological parameter constraints from tomographic weak gravitational lensing. *Mon. Not. Roy. Astron. Soc.* **465**, 1454–1498 (2017).
15. Joudaki, S. et al. KiDS-450: testing extensions to the standard cosmological model. *Mon. Not. Roy. Astron. Soc.* **471**, 1259–1279 (2017).
16. Motloch, P. & Hu, W. Tensions between direct measurements of the lens power spectrum from Planck data. *Phys. Rev. D* **97**, 103536 (2018).
17. Charnock, T., Battye, R. A. & Moss, A. Planck data versus large scale structure: methods to quantify discordance. *Phys. Rev. D* **95**, 123535 (2017).
18. Raveri, M. & Hu, W. Concordance and discordance in cosmology. *Phys. Rev. D* **99**, 043506 (2019).
19. Adhikari, S. & Huterer, D. A new measure of tension between experiments. *J. Cosmol. Astropart. Phys.* **1901**, 036 (2019).
20. Bernal, J. L., Verde, L. & Riess, A. G. The trouble with H_0. *J. Cosmol. Astropart. Phys.* **1610**, 019 (2016).
21. Zhao, G. B. et al. Dynamical dark energy in light of the latest observations. *Nat. Astron.* **1**, 627–632 (2017).
22. Di Valentino, E., Melchiorri, A., Linder, E. V. & Silk, J. Constraining dark energy dynamics in extended parameter space. *Phys. Rev. D* **96**, 023523 (2017).
23. Poulin, V., Smith, T. L., Karwal, T. & Kamionkowski, M. Early dark energy can resolve the Hubble tension. *Phys. Rev. Lett.* **122**, 221301 (2019).
24. Yang, W., Pan, S., Di Valentino, E., Saridakis, E. N. & Chakraborty, S. Observational constraints on one-parameter dynamical dark-energy parametrizations and the H_0 tension. *Phys. Rev. D* **99**, 043543 (2019).
25. Bond, J. R., Efstathiou, G. & Tegmark, M. Forecasting cosmic parameter errors from microwave background anisotropy experiments. *Mon. Not. Roy. Astron. Soc.* **291**, L33–L41 (1997).
26. Efstathiou, G. & Bond, J. R. Cosmic confusion: degeneracies among cosmological parameters derived from measurements of microwave background anisotropies. *Mon. Not. Roy. Astron. Soc.* **304**, 75–97 (1999).
27. Elgaroy, O. & Multamaki, T. On using the CMB shift parameter in tests of models of dark energy. *Astron. Astrophys.* **471**, 65–70 (2007).
28. Hinshaw, G. et al. Nine-year Wilkinson Microwave Anisotropy Probe (WMAP) observations: final maps and results. *Astrophys. J. Suppl.* **208**, 25 (2013).
29. Spiegelhalter, D., Best, N. G., Carlin, B. P. & van der Linde, A. Bayesian measures of model complexity and fit. *J. R. Stat. Soc. B* **64**, 583–639 (2002).
30. Trotta, R. Bayes in the sky: Bayesian inference and model selection in cosmology. *Contemp. Phys.* **49**, 71–104 (2008).
31. Liddle, A. R. Information criteria for astrophysical model selection. *Mon. Not. Roy. Astron. Soc.* **377**, L74–L78 (2007).
32. Verdinelli, I. & Wasserman, L. Computing Bayes factors using a generalization of the Savage–Dickey density ratio. *J. Am. Stat. Assoc.* **90**, 614–618 (1995).
33. Trotta, R. Applications of Bayesian model selection to cosmological parameters. *Mon. Not. Roy. Astron. Soc.* **378**, 72–82 (2007).
34. Ade, P. A. R. et al. (Planck Collaboration) Planck 2015 results. XIII. Cosmological parameters. *Astron. Astrophys.* **594**, A13 (2016).
35. Addison, G. E. et al. Quantifying discordance in the 2015 Planck CMB spectrum. *Astrophys. J.* **818**, 132 (2016).
36. Beutler, F. et al. The 6dF Galaxy Survey: baryon acoustic oscillations and the local Hubble constant. *Mon. Not. Roy. Astron. Soc.* **416**, 3017–3032 (2011).
37. Ross, A. J. et al. The clustering of the SDSS DR7 main galaxy sample—I. A 4 per cent distance measure at $z = 0.15$. *Mon. Not. Roy. Astron. Soc.* **449**, 835–847 (2015).
38. Alam, S. et al. The clustering of galaxies in the completed SDSS-III Baryon Oscillation Spectroscopic Survey: cosmological analysis of the DR12 galaxy sample. *Mon. Not. Roy. Astron. Soc.* **470**, 2617–2652 (2017).
39. Aghanim, N. et al. (Planck Collaboration) Planck 2018 results. VIII. Gravitational lensing. Preprint at https://arxiv.org/abs/1807.06210 (2019).
40. Abbott, T. M. C. et al. (Dark Energy Survey and South Pole Telescope Collaborations) Dark Energy Survey Year 1 results: a precise H_0 measurement from DES Y1, BAO, and D/H data. *Mon. Not. Roy. Astron. Soc.* **480**, 3879–3888 (2018).
41. Hikage, C. et al. Cosmology from cosmic shear power spectra with Subaru Hyper Suprime-Cam first-year data. *Publ. Astron. Soc. Jpn* **71**, 43 (2019).
42. Schlaufman, K. C., Thompson, I. B. & Casey, A. R. An ultra metal-poor star near the hydrogen-burning limit. *Astrophys. J.* **867**, 98 (2018).
43. Bond, H. E., Nelan, E. P., VandenBerg, D. A., Schaefer, G. H. & Harmer, D. HD 140283: a star in the solar neighborhood that formed shortly after the big bang. *Astrophys. J.* **765**, L12 (2013).
44. Jimenez, R., Cimatti, A., Verde, L., Moresco, M. & Wandelt, B. The local and distant Universe: stellar ages and H0. *J. Cosmol. Astropart. Phys.* **3**, 043 (2019).
45. Cyr-Racine, F. Y., de Putter, R., Raccanelli, A. & Sigurdson, K. Constraints on large-scale dark acoustic oscillations from cosmology. *Phys. Rev. D* **89**, 063517 (2014).
46. Blennow, M., Fernandez-Martinez, E., Mena, O., Redondo, J. & Serra, P. Asymmetric dark matter and dark radiation. *J. Cosmol. Astropart. Phys.* **1207**, 022 (2012).
47. Mangano, G., Melchiorri, A., Serra, P., Cooray, A. & Kamionkowski, M. Cosmological bounds on dark matter–neutrino interactions. *Phys. Rev. D* **74**, 043517 (2006).
48. Leonard, C. D., Bull, P. & Allison, R. Spatial curvature endgame: reaching the limit of curvature determination. *Phys. Rev. D* **94**, 023502 (2016).
49. Bull, P., Ferreira, P. G., Patel, P. & Santos, M. G. Late-time cosmology with 21 cm intensity mapping experiments. *Astrophys. J.* **803**, 21 (2015).
50. Lewis, A. & Bridle, S. Cosmological parameters from CMB and other data: a Monte Carlo approach. *Phys. Rev. D* **66**, 103511 (2002).
51. Scolnic, D. M. et al. The complete light-curve sample of spectroscopically confirmed SNe Ia from Pan-STARRS1 and cosmological constraints from the combined Pantheon sample. *Astrophys. J.* **859**, 101 (2018).
52. Cooke, R. J., Pettini, M. & Steidel, C. C. One percent determination of the primordial deuterium abundance. *Astrophys. J.* **855**, 102 (2018).
53. Kazin, E. A. et al. The WiggleZ Dark Energy Survey: improved distance measurements to $z = 1$ with reconstruction of the baryonic acoustic feature. *Mon. Not. Roy. Astron. Soc.* **441**, 3524–3542 (2014).
54. Abbott, T. M. C. et al. (Dark Energy Survey Collaboration) Dark Energy Survey Year 1 results: measurement of the baryon acoustic oscillation scale in the distribution of galaxies to redshift 1. *Mon. Not. Roy. Astron. Soc.* **483**, 4866–4883 (2019).
55. Bautista, J. E. et al. Measurement of baryon acoustic oscillation correlations at $z = 2.3$ with SDSS DR12 Lyα-Forests. *Astron. Astrophys.* **603**, A12 (2017).
56. Ata, M. et al. The clustering of the SDSS-IV extended Baryon Oscillation Spectroscopic Survey DR14 quasar sample: first measurement of baryon acoustic oscillations between redshift 0.8 and 2.2. *Mon. Not. Roy. Astron. Soc.* **473**, 4773–4794 (2018).
57. du Mas des Bourboux, H. et al. Baryon acoustic oscillations from the complete SDSS-III Lyα-quasar cross-correlation function at $z = 2.4$. *Astron. Astrophys.* **608**, A130 (2017).

Acknowledgements
E.D.V. acknowledges support from the European Research Council in the form of a Consolidator Grant with number 681431. A.M. thanks the University of Manchester and the Jodrell Bank Centre for Astrophysics for hospitality. A.M. is supported by TAsP, iniziativa specifica INFN. We thank M. Melchiorri for discussions.

Author contributions
E.D.V. performed all MCMC analyses, simulations and the Planck parameters analysis at different scales, produced all the figures, wrote the paper and helped with additional ideas. A.M. proposed the main idea, performed the tension analyses and wrote the paper. J.S. wrote the paper and helped with additional ideas.

Competing interests
The authors declare no competing interests.

Additional information
Correspondence and requests for materials should be addressed to A.M.